

Thermal convection in a horizontal plane Couette flow

By ROBERT P. DAVIES-JONES†

National Center for Atmospheric Research, Boulder, Colorado 80302, U.S.A.

(Received 18 November 1970)

We investigate the behaviour of infinitesimal perturbations introduced into an unstably stratified horizontal Couette flow. We assume that the fluid is Boussinesq and contained in an infinite conducting rectangular channel which is uniformly heated from below. The sidewalls are rigid and the Couette flow is generated by moving them with equal and opposite velocities along the channel. The top and bottom are assumed to be free so that we can separate variables.

Without shear, the preferred modes of convection closely resemble transverse ‘finite rolls’ (Davies-Jones 1970). Shear increases the critical wavelength so that the preferred modes become longitudinally elongated cells, or even longitudinal rolls in some cases. The critical Rayleigh number increases quite rapidly at first with Reynolds number, but at higher Reynolds numbers it levels off to a constant value (which cannot be greater than the shear-independent Rayleigh number at which longitudinal disturbances first become unstable).

We also find that the disturbances are tilted in the same direction as the shear, and that the marginally stable ones transfer kinetic energy from the mean flow to the perturbations. Except at low Reynolds numbers, the long wave perturbations gain more energy through the conversion of mean flow kinetic energy than through the release of potential energy, even though the instability is convective in origin.

1. Introduction

In a previous paper (Davies-Jones 1970) we investigated the stability of a Boussinesq fluid heated from below in an infinite rectangular channel with no-slip sidewalls and free top and bottom. The cells which appear at the onset of convection were found to closely resemble transverse rolls [in agreement with Davis (1967)]. In this paper we extend this work by including horizontal shear which is generated by moving the sidewalls at a constant rate in opposite directions.

The stability of the unstratified problem (viscous plane Couette flow) has been investigated most recently by Gallagher & Mercer (1962, 1964) and Deardorff (1963). Deardorff concluded that the flow was definitely stable to infinitesimal disturbances up to a Reynolds number of 1430. The trend of their results suggest that it is stable to small perturbations at all Reynolds numbers.

Studies of stratified Couette flow where the shear is vertical have been made

† Present address: The National Severe Storms Laboratory, Norman, Oklahoma 73069.

by Gallagher & Mercer (1965), Deardorff (1965) and Asai (1970), among others. Their problem differs from ours in an important aspect (apart from the orientation of the shear); namely, the fluid is unbounded horizontally. They found that the preferred modes of convection are longitudinal rolls (i.e. rolls parallel to the mean flow). Asai showed that longitudinal rolls gain energy from the mean flow, but transverse rolls lose energy to the mean flow.

The mathematical approach that we use here is similar to the one used by Gallagher & Mercer (1962, 1965), except that we compute the eigenfunctions as well as the eigenvalues.

2. Mathematical formulation

We use the following notation: x and y are the horizontal co-ordinates along and across the channel and z is the vertical co-ordinate. The subscript $*$ refers to dimensional quantities. The planes $z_* = 0, 2h_*$ and $y_* = \pm b_*$ define the channel. u_*, v_* and w_* are the components of velocity in the x, y and z directions, p_* is the pressure ρ_* is the density, θ_* is the temperature measured with respect to the average temperature, g_* is the acceleration due to gravity, and α_*, ν_* and κ_* are the coefficients of volume expansion, kinematic viscosity and thermal diffusivity.

We assume that the unperturbed mean flow, \bar{u}_* , is one of constant horizontal shear, u_{0*} (i.e. $\bar{u}_* = u_{0*}y_*$). The vertical temperature gradient, β_* , is constant as it is established by heat conduction.

Infinitesimal perturbations, denoted by primes, are introduced into the system. If they grow with time, the initial equilibrium is unstable. We assume that the applied temperature difference is small enough so that we can use the Boussinesq approximation (i.e. $|\alpha_*\theta_*| \ll 1$). We define dimensionless variables (non-subscripted) as follows.

$$\begin{aligned} x, y, z &\equiv b_*^{-1}[x_*, y_*, z_*], \\ t &\equiv \kappa_* b_*^{-2} t_*, \\ u', v', w' &\equiv b_* \kappa_*^{-1}[u'_*, v'_*, w'_*], \\ \theta' &\equiv -\beta_*^{-1} b_*^{-1} \theta'_*, \\ p' &\equiv \rho_{0*}^{-1} b_*^2 \kappa_*^{-2} p'_*, \end{aligned}$$

where ρ_{0*} is the mean density of the fluid in the channel. The linearized perturbation equations are then

$$\mathcal{L}_1 u' + Pr Re v' = -\partial p' / \partial x, \quad (1)$$

$$\mathcal{L}_1 v' = -\partial p' / \partial y, \quad (2)$$

$$\mathcal{L}_1 w' = -\frac{\partial p'}{\partial z} + \frac{Pr Ra}{16A^4} \theta', \quad (3)$$

$$\frac{\partial u'}{\partial x} + \frac{\partial v'}{\partial y} + \frac{\partial w'}{\partial z} = 0, \quad (4)$$

$$\mathcal{L}_2 \theta' - w' = 0, \quad (5)$$

where \mathcal{L}_1 and \mathcal{L}_2 denote the differential operators $[\partial/\partial t + Pr Re y(\partial/\partial x) - Pr \nabla^2]$ and $[\partial/\partial t + Pr Re y(\partial/\partial x) - \nabla^2]$, $Pr = \nu_*/\kappa_*$ is the Prandtl number,

$$Ra = -g_* \alpha_* \beta_* (2h_*)^4 / \kappa_* \nu_*$$

is the Rayleigh number, $Re = u_{0*} b_*^2 / \nu_*$ is the Reynolds number, and A is the height-to-width ratio of the channel ($\equiv h_*/b_*$).

We assume that the top and bottom are free and perfect conductors so that

$$\theta' = w' = \partial u' / \partial z = \partial v' / \partial z = 0 \quad \text{at } z = 0, 2A \tag{6}$$

and that the sides are rigid and perfectly conducting so that

$$u' = v' = w' = \theta' = 0 \quad \text{at } y = \pm 1. \tag{7}$$

(Perfectly conducting sides are chosen so that we can expand θ' in an infinite sine series later on.)

From (4) and (5) the latter are equivalent to

$$v' = \partial v' / \partial y = \theta' = \mathcal{L}_2 \theta' = 0 \quad \text{at } y = \pm 1, \tag{8}$$

but cannot be expressed simply in terms of either v' alone or θ' alone.

The boundary conditions (6) allow us to separate variables by assuming that

$$\left. \begin{aligned} u'(x, y, z, t) \\ v'(x, y, z, t) \\ p'(x, y, z, t) \\ w'(x, y, z, t) \\ \theta'(x, y, z, t) \end{aligned} \right\} = \left. \begin{aligned} \hat{u}(y) \\ \hat{v}(y) \\ \hat{p}(y) \\ \hat{w}(y) \\ \hat{\theta}(y) \end{aligned} \right\} \left. \begin{aligned} e^{\sigma t} e^{ikx} \cos mz, \\ e^{\sigma t} e^{ikx} \sin mz, \end{aligned} \right\} \tag{9}$$

where $\sigma (\equiv \sigma_r + i\sigma_i)$ is the complex growth rate of the normal mode disturbance with x wave-number k and vertical wave-number $m (= q\pi/2A; q = 1, 2, 3, \dots)$. We assume henceforth that $q = 1$ since this gives the most unstable mode.

The perturbation energy equation shows how the various forms of energy – namely, potential, perturbation kinetic and mean flow kinetic – can be transformed into each other. We obtain this equation by multiplying the real parts of (1), (2) and (3) by $\text{Re}(u')$, $\text{Re}(v')$, and $\text{Re}(w')$ respectively, averaging the equations over one wavelength in x , adding the equations together and integrating over the cross-sectional area, S , of the channel (the averaging operator is denoted below by a bar). This gives after frequency integration by parts and use of the boundary conditions,

$$\begin{aligned} \frac{1}{2} \frac{\partial}{\partial t} \iint (\overline{u'^2} + \overline{v'^2} + \overline{w'^2}) dS &= \{\bar{K} \cdot K'\} + \{P \cdot K'\} \\ &\quad - Pr \iint \{\overline{\nabla u' \cdot \nabla u'} + \overline{\nabla v' \cdot \nabla v'} + \overline{\nabla w' \cdot \nabla w'}\} dS, \end{aligned} \tag{10}$$

where the last term clearly represents the loss of energy through viscous dissipation, and

$$\{\bar{K} \cdot K'\} = -Pr Re \iint \overline{u'v'} dS, \tag{11}$$

$$\{P \cdot K'\} = \frac{Pr Ra}{16A^4} \iint \overline{w'\theta'} dS \tag{12}$$

represent the conversion of mean kinetic energy and potential energy into perturbation kinetic energy [as shown, for example, in Davies-Jones (1969)].

3. Longitudinal disturbances

We can make some interesting deductions about longitudinal disturbances (i.e. those with no variations along the channel) without proceeding further. Since (2), (3), (4), (5) and the boundary conditions are independent of u' and Re in this case, we can solve these four equations for the eigenvalue (Ra or σ) and the eigenfunctions v' , w' , θ' and p' and they must all be independent of Re . Furthermore, when $\partial/\partial t = 0$ we deduce that they are also independent of Pr (except for p'). Thus, longitudinal disturbances become unstable at the same Rayleigh number for all shears and Prandtl numbers, and their growth rate, σ , at a given Rayleigh number also has no Reynolds number dependence (but does depend on Pr).

It follows from (1) that u' varies linearly with Re , and is also independent of Pr when $\sigma = 0$. Hence $\{\bar{K}.K'\} \propto Re^2$ and $\{P.K'\} \propto Re^0$, and both vary as Pr when $\sigma = 0$. Thus, above a certain Reynolds number the perturbations gain (or lose) more energy through conversion of mean kinetic energy than they gain through conversion of potential energy.

We can also show that unstable or marginally stable longitudinal disturbances ($\sigma \geq 0$) and even slowly-decaying ones (those for which $\sigma + Pr m^2 > 0$) convert mean kinetic energy into perturbation kinetic energy. The proof is as follows. By multiplying (1) by u' , integrating over S and using (9) we obtain

$$\{\bar{K}.K'\} = \iiint \left\{ (\sigma + Pr m^2) u'^2 + Pr \left(\frac{\partial u'}{\partial y} \right)^2 \right\} dS. \tag{13}$$

Thus $\{\bar{K}.K'\}$ is always positive when $\sigma + Pr m^2 > 0$ (since with $k = 0$ we can assume all the variables are real). Note that the Re^2 dependence of $\{\bar{K}.K'\}$ has no effect on the stability of the disturbances because the loss of energy through dissipation by the x component of the viscous force also varies as Re^2 .

4. Solution by Galerkin's technique

By elimination of variables in (1)–(5) we obtain the following two independent simultaneous differential equations in v' and θ' :

$$\mathcal{L}_1 \nabla^2 v' + \frac{Pr Ra}{16A^4} \frac{\partial^2 \theta'}{\partial y \partial z} = 0, \tag{14}$$

$$\left(\frac{\partial}{\partial y} \mathcal{L}_1 - 2 Pr Re \frac{\partial}{\partial x} \right) \frac{\partial v'}{\partial z} = \left[\frac{Pr Ra}{16A^4} \frac{\partial^2}{\partial x^2} - \mathcal{L}_1 \mathcal{L}_2 \left(\frac{\partial^2}{\partial x^2} + \frac{\partial^2}{\partial z^2} \right) \right] \theta'. \tag{15}$$

We reduce (14) and (15) to ordinary differential equations in $\hat{\theta}$ and \hat{v} by separating variables according to (9). We also use the transformation $y_1 = \frac{1}{2}\pi(y + 1)$, and define new parameters

$$\left. \begin{aligned} \lambda_1 &= -4\alpha^2 Pr/\pi^2 + (4/\pi^2) (ik Pr Re - \sigma), \\ \lambda_2 &= -4\alpha^2/\pi^2 + (4/\pi^2) (ik Pr Re - \sigma). \end{aligned} \right\} \tag{16}$$

Suitable expansions for $\hat{\theta}$ and \hat{v} which satisfy the boundary conditions (8) have been given by Gallagher & Mercer (1962, 1965). They are

$$\hat{\theta} = \sum_{r=1}^{\infty} b_r \sin ry_1, \tag{17}$$

$$\hat{v} = \sum_{r=1}^{\infty} a_r Y_r(y_1), \tag{18}$$

where the Y_r are the eigenfunctions of the boundary-value problem

$$d^4 Y/dy^4 = \mu^4 Y; \quad Y = dY/dy = 0 \quad \text{at} \quad y = 0, \pi. \tag{19}$$

We use Galerkin's method to replace the differential equations by a set of algebraic equations whose solutions are the coefficients of complete orthogonal expansions. This is done by truncating the above expansions after N terms, and making the truncation errors in (14) and (15) orthogonal to each of the first N terms in (20) and (19) respectively, thereby obtaining a set of $2N$ algebraic equations. This procedure is the same as used by Gallagher & Mercer (1965).

4.1. *Computation of the eigenvalues*

The final equations may be written in matrix form as follows:

$$(A_1 \lambda_1 + A_0) a = Ra Bb, \tag{20}$$

$$(C_1 \lambda_1 + C_0) a = (D_2 \lambda_1 \lambda_2 + D_{11} \lambda_1 + D_{12} \lambda_2 + D_0 + Ra E) b, \tag{21}$$

where $A_1, A_0, B, C_1, C_0, D_2, D_{11}, D_{12}, D_0$ and E are infinite square matrices whose elements are independent of Ra, λ_1 and λ_2 , and a and b are infinite column matrices whose elements are the coefficients a_r and b_r respectively.

We also define $A \equiv A_1 \lambda_1 + A_0, C \equiv C_1 \lambda_1 + C_0, D \equiv D_2 \lambda_1 \lambda_2 + D_{11} \lambda_1 + D_{12} \lambda_2 + D_0$ for later use. Eliminating b yields

$$(A_1 \lambda_1 + A_0) a = Ra B(D_2 \lambda_1 \lambda_2 + D_{11} \lambda_1 + D_{12} \lambda_2 + D_0 + Ra E)^{-1} (C_1 \lambda_1 + C_0) a. \tag{22}$$

When $Ra = 0$ the problem reverts to that of three-dimensional unstratified plane Couette flow (or two-dimensional if m is set equal to zero). Then λ_1 is clearly the eigenvalue and a the eigenvector of $-A_1^{-1} A_0$ [a result first derived by Gallagher & Mercer (1962)].

In stratified cases we have the option of regarding Ra as the eigenvalue of the boundary-value problem with k, A, Pr, Re and σ as parameters or of treating σ as the eigenvalue with Ra as one of the parameters. We shall adopt each approach in turn.

In determining the stability boundary (locus of $\sigma_r = 0$) it is convenient to regard Ra as the eigenvalue. In this case we find from (22) that Ra is the eigenvalue and a the eigenvector of $(C - EB^{-1}A)^{-1} DB^{-1}A$. The eigenvalues and eigenvectors of this matrix are generated by the QR -algorithm (Francis 1961, 1962) and inverse iteration (Wilkinson 1965), respectively. b can then be obtained from (21).

We assume initially that σ is zero on the stability boundary. In some cases, as Re or k is increased the lowest eigenvalue becomes complex which is physically

meaningless since Ra must be real. In such cases the critically stable modes occur in transitive pairs, i.e. with phase velocities $\pm \sigma_i/k$, which we locate by varying $|\sigma_i|$ until we find the value for which the lowest eigenvalue is real.

We now adopt the other approach in which σ is regarded as the eigenvalue. Assuming $Pr = 1$ yields a great simplification since then

$$\lambda_1 = \lambda_2 \quad (\equiv \lambda \text{ when } Pr = 1)$$

and we can rewrite (22) in the form

$$(P\lambda^3 + Q\lambda^2 + R\lambda + S)a = 0. \tag{23}$$

Provided that P is non-singular, we can easily find a $3N \times 3N$ matrix, Λ , of which λ is the eigenvalue and

$$\begin{bmatrix} a \\ \dots \\ \lambda a \\ \dots \\ \lambda^2 a \end{bmatrix}$$

is the eigenvector (written in partitioned form). λ is found by the QR -algorithm. We could in principle determine the eigenvectors of Λ and hence obtain a but a much more economical method in terms of time and computer storage is to again compute a as the eigenvector of $(C - EB^{-1}A)^{-1}DB^{-1}A$.

Care must be taken to avoid spurious eigenvalues. For example, note that the limit $Ra \rightarrow 0$ is singular because the matrices P and Q do not vanish in this limit as they should do according to (22). Consequently, $2N$ spurious eigenvalues enter as we approach the unstratified limit.

4.2. *Computation of the eigenfunctions*

Having computed the a 's and b 's, we evaluate θ and \hat{v} from (17) and (18).

In determining the other dependent variables we avoid term by term differentiations of (17) and (18) [which yield series which, if they converge at all, do so much slower than the original series] by performing numerical integrations of the relevant differential equations. We define grid points across the channel by

$$y_j = -1 + jh \quad (j = -1, 0, 1, \dots, J + 1),$$

where $h = 2/J$. The exterior points y_{-1}, y_{J+1} are used to satisfy boundary conditions.

We determine \hat{p} by integrating the divergence equation

$$\frac{d^2\hat{p}}{dy^2} - (k^2 + m^2)\hat{p} = -2ikPrRe\hat{v} + \frac{mPrRa}{16A^4}\hat{\theta}$$

subject to the boundary conditions $d\hat{p}/dy = Pr(d^2\hat{v}/dy^2)$ at $y = \pm 1$, obtained by putting $\hat{v} = 0$ in (2). After first making a transformation of dependent variable to reduce this to a one point boundary-value problem, we use the Runge-Kutta technique with error control to generate the solutions.

\hat{u} and \hat{w} are obtained by writing the x - and z -equations of motion in finite difference forms, and solving for $\hat{u}(y_j)$ and $\hat{w}(y_j)$ by Gaussian elimination after applying the boundary conditions $\hat{u} = \hat{w} = 0$ at $y = \pm 1$.

Lastly, we compute the divergence to give us a measure of the error in the solutions, and evaluate the Reynolds stresses, heat transports and rates of energy conversions.

4.3. *Convergence of the series*

As we go to higher values of the Reynolds or Rayleigh number, we need to increase the number of terms, N , in the series for \hat{v} and $\hat{\theta}$ to attain the same accuracy. The reason for this has been given by Gallagher & Mercer (1962).

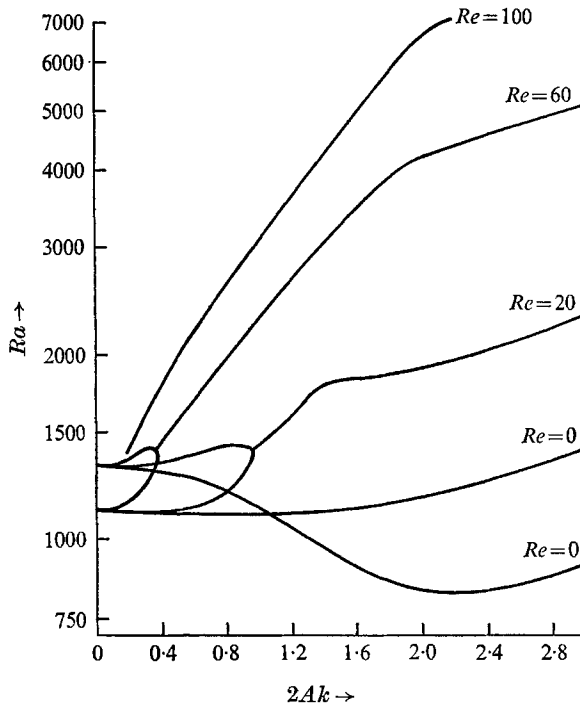


FIGURE 1. The Rayleigh number of the two lowest modes at marginal stability as a function of $2Ak$ for various Reynolds numbers in the case $Pr = 0.7$, $A = 0.5$.

As is usual in boundary-value problems the computed eigenvalues are much more accurate than the computed eigenfunctions. For instance, after retaining just ten terms in each series we find that for $A = 0.5$, $Pr = 1.0$, $k = 2.0$, $Re = 62$, the method with Ra as the eigenvalue yields $Ra = 4997$, $\sigma_r = 67.4$ for $\sigma_i = 0$ compared to $Ra = 5000$, $\sigma_r = 67.4$ as given by the ‘ σ method’. However, we chose $N = 30$ and $J = 50$ so that we could compute the eigenfunctions accurately enough for the divergence to be about one order of magnitude smaller than the individual terms in the continuity equation.

5. The results

5.1. *The stability boundary*

Calculations were performed for three Prandtl numbers, $Pr = 0.01$ (indicative of a low Prandtl number), 0.7 (air at room temperature) and 6.0 (water at 28°C). Figure 1 shows the Rayleigh number at marginal stability ($\sigma_r = 0$) as a function

of $2Ak$ (i.e. the x wave-number in units of the inverse of the channel height) for the two lowest modes at various Reynolds numbers for $Pr = 0.7$ and $A = 0.5$. For no shear the curves for the two modes cross, but for $Re = 20$ (and higher values) the curves join to form a single curve along which the two modes are a

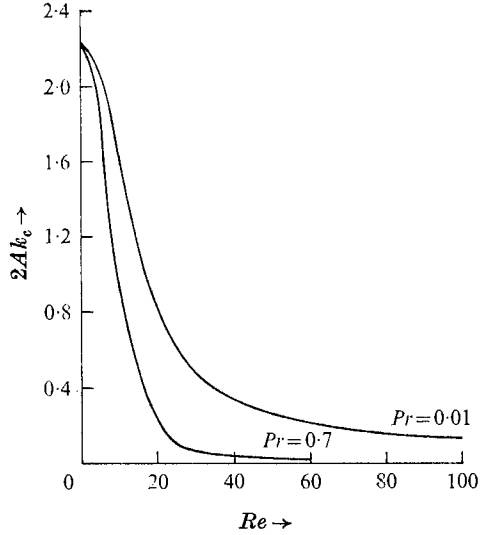


FIGURE 2. Critical wave-number (in units of the inverse channel height) versus Reynolds number for $A = 0.5$ and various Prandtl numbers.

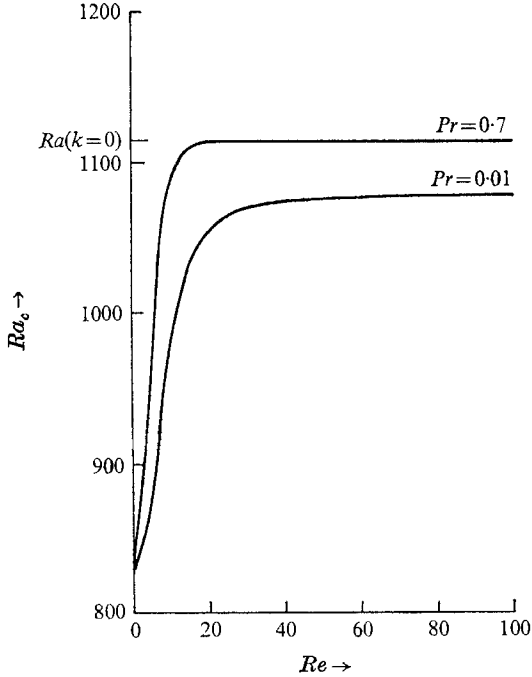


FIGURE 3. Critical Rayleigh number versus Reynolds number for $A = 0.5$ and various Prandtl numbers.

transitive pair with equal but opposite phase velocities. For the sake of clarity only the common branch of the curves for $Re = 100$ has been included. We have shown that the stability of longitudinal ($k = 0$) disturbances is not affected by shear. It is apparent that other disturbances are generally stabilized by shear, and hence that the critical wave-number (i.e. the wave-number that appears at the onset of convection) decreases with increasing Reynolds number.

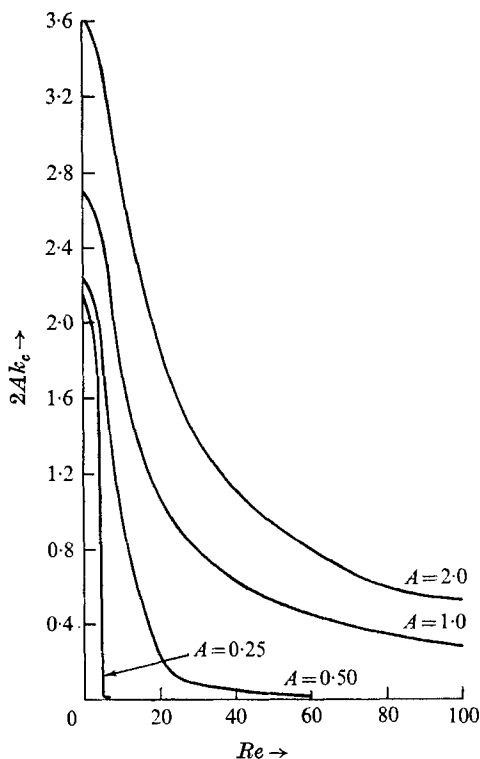


FIGURE 4. Critical wave-number (in units of the inverse channel height) versus Reynolds number for $Pr = 0.7$ and various aspect ratios.

Figures 2 and 3 show the critical wave-number, $2Ak_c$, and Rayleigh number, Ra_c , as functions of the Reynolds number for $Pr = 0.01$ and 0.7 and a fixed aspect ratio ($A = 0.5$). For $Re = 0$ it is well known that Ra_c and k_c are independent of Pr . For $Pr = 0.7$ the critical wave-number quickly approaches zero and the critical Rayleigh number reaches the value of Ra at which longitudinal rolls become unstable (indicated by the hatchmark on the axis and hereafter referred to as the ' $k = 0$ value') and levels off. For $Pr = 6$ these limits are attained so rapidly that the ascending or descending parts of the curves coincide with the ordinate axes. For $Pr = 0.01$ the curves level off before reaching these limits.

Figures 4 and 5 show the same curves for $Pr = 0.7$ and different aspect ratios. We have indicated the $k = 0$ values (which increase with A because of the greater importance of the side boundary layers) for $A = 0.25, 0.5, 1.0$ and 2.0 by the

four hatchmarks on the ordinate axis in figure 5. For $A = 0.25$ and 0.5 , the critical wave-number and Rayleigh number tend to zero and the $k = 0$ value, respectively, but for $A = 1.0$ and 2.0 the curves level off before reaching these values. [The critical Rayleigh number curve for $A = 1.0$ actually has a slight

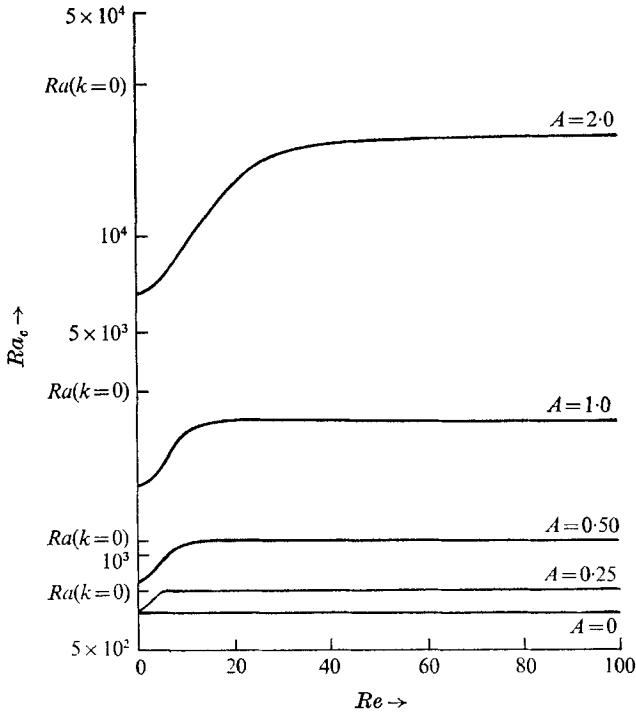


FIGURE 5. Critical Rayleigh number versus Reynolds number for $Pr = 0.7$ and various aspect ratios.

maximum at $Re = 23$ before levelling off.] Thus, at high aspect ratios or low Prandtl numbers long cells rather than rolls are preferred in the high Reynolds number limit. In the high aspect ratio case the longitudinal rolls suffer sufficient viscous damping in the side boundary layers to prevent their appearance at the onset of convection.

5.2. Growth rate curves

Growth rate curves (as functions of the Reynolds number for given Ra and k) are given in Davies-Jones (1969). They show the general stabilizing influence of the shear on the disturbances, and the transitive nature of the disturbances at high Reynolds numbers. The phase velocities increase in magnitude monotonically with k and Re but depend only slightly on Ra .

5.3. The structures and energy conversion properties of the cells

Shear has the effect on all marginally stable perturbations of establishing a negative correlation between u' and v' , and tilting the isopleths of w' , θ' and p' in the direction of the shear (except for the isobars near the sidewalls which are

tilted in the opposite sense). Exceptions to this rule are longitudinal rolls where (naturally) the isopleths are always parallel to the sidewalls, and transitive disturbances where the isobars are sometimes tilted in the opposite sense. In general, the tilt of the vertical velocity and temperature fields is apparently caused by advection, and the tilt of the isobars by adjustment to the above fields. The direction of the pressure forces is therefore generally such as to give rise to a negative horizontal Reynolds stress. Since the inertia force, $-Pr Re v'$, acting in the x direction enhances this effect, it is not surprising that $\overline{u'v'}$ is negative on the (cross-channel) average.

We define an energy conversion ratio, $\mathcal{R} \equiv \{\overline{K} \cdot K'\} / \{P \cdot K'\}$, which is free of the arbitrary constant which enters into any linear, homogeneous boundary-value problem such as this one. \mathcal{R} is the ratio of the rates of exchange between mean flow and perturbation kinetic energy and between potential and perturbation kinetic energy. We showed in § 3 for longitudinal rolls that $\mathcal{R} \propto Re^2$ and that \mathcal{R} is positive and independent of Pr when $\sigma = 0$. At marginal stability \mathcal{R} attains unity at some Reynolds number in the range 10–25 for aspect ratios, A , in the range 0.5–4.0. Thus, at higher Reynolds numbers, the perturbations gain more energy from the mean flow than they do from the release of potential energy.

We now consider the effect of varying the Rayleigh number on the structure of longitudinal rolls. Without shear the horizontal paths of the fluid particles are perpendicular to the sidewalls. We can deduce from (1) with $\partial/\partial x = 0$ that the inertia force, $-Pr Re v'$, deflects the fluid particles to the left when $\sigma > 0$ or the viscous term, $Pr \nabla^2 u'$, dominates the local acceleration, $\partial u'/\partial t$. However, for rapidly decaying modes where the local acceleration is the dominant term, the inertia force deflects the particles to the right, thereby inducing a positive, rather than negative, horizontal Reynolds stress. The transition between these two cases occurs at $Ra \approx 75$.

These results indicate that unstable stratification acts as a catalyst as far as release of mean flow kinetic energy is concerned. Without stratification the mean flow gains energy from the longitudinal perturbations, but with the presence of a small amount of unstable stratification, this energy conversion is reversed, and except at low Reynolds numbers, the perturbations actually 'feed' more on the mean flow than on the potential energy of the system. Of course, the perturbations cannot sustain themselves, and cause the Couette flow to become unstable until the critical Rayleigh number is reached.

In the absence of shear, the preferred modes of convection closely resemble 'finite rolls' aligned perpendicular to the side-walls (Davies-Jones 1970). Finite rolls are defined as "cells with (only) two non-zero velocity components dependent on all three spatial variables" [see Davis 1967]. As previously stated, shear tilts the preferred modes in the downstream direction and increases their wavelength. As a result we find that for $Re \gtrsim 30$, \mathcal{R} is generally greater than unity. \mathcal{R} increases with decreasing A or increasing Pr at a given Reynolds number because of increasing cell elongation (see figure 2 and 4).

As we proceed in the direction of increasing k (keeping A , Pr , Re fixed) along the stability boundary, \mathcal{R} decreases rapidly near $k = 0$ but much more slowly at higher k . \mathcal{R} is positive in all the stationary cases we computed. We attribute the

stabilization of the short wave disturbances as due to the fluid particles traversing diagonal horizontal paths instead of ones which are nearly parallel to the sidewalls. All the fluid particles thus approach closer to the sidewalls in some part of their trajectories, and hence are slowed down, assuming that their viscous retardation increases more than linearly with $|y|$.

We did not evaluate \mathcal{R} for transitive modes because, if allowance is made for the interaction between the co-existing members of a transitive pair, \mathcal{R} becomes a periodic function of time instead of a constant. However, we find that $\{\bar{K}, K'\}$ is positive for each separate member. In addition, with increasing wave-number or Reynolds number these disturbances become more decoupled from their associates in the transitive pair by becoming more localized on the side of the channel where the phase velocity assumes the value of the mean flow. This decoupling phenomenon at short wavelength has been described by Howard (1963) in connexion with a flow composed of a pair of shear layers with discontinuities in density as well as in mean flow at the interfaces. The disturbances become more stable at higher values of k and Re because of the increased internal dissipation associated with the localization.

For unstratified three-dimensional Couette flow with $A = 0.5$, $Re = 10$ (no other cases were computed) we find that perturbation kinetic energy is converted into kinetic energy of the mean flow for $k = 0.5$ and 1.0 but the conversion is in the opposite sense at $k \gtrsim 1.5$. Even though they gain energy from the mean flow, the short wave perturbations decay because of strong viscous damping. Shortly above $k = 2.0$ the disturbances become transitive and begin to localize on one side of the channel. The w' and p' isopleths once more slope with the shear, except in one instance ($k = 0.5$) where the w' isopleths slope in the opposite direction. The pressure gradient force thus acts in such a direction as to give a negative Reynolds stress. However, at short wavelengths, the inertia force, $-Pr Re v'$, which deflects particles to the right since the disturbances are rapidly decaying (in the sense defined previously), dominates the pressure gradient force, and produces a positive Reynolds stress, and hence an energy loss by the perturbations to the mean flow.

6. Summary and comparison with the vertical shear problem

We find that short-wavelength disturbances are stabilized by the shear. (This is analogous to the stabilization of transverse rolls by vertical shear.) The critical Rayleigh number is never greater than the lowest Rayleigh number at which a longitudinal disturbance can become unstable, the latter being independent of shear (as in the vertical shear case). The preferred mode of convection is, thus, always a longitudinally elongated cell but, because of the influence of the sidewalls, it may not become a longitudinal roll in the high Reynolds number limit. This is in contrast to the vertical shear problem (without sidewalls) where the most unstable mode is always a longitudinal roll. As is typical of Couette flow problems, the short wave disturbances occur in pairs which propagate along the channel in opposite directions when shear is present.

For both shear orientations, the isopleths of w' , θ' and p' tilt in the direction

of the shear. Asai (1970) finds, however, that with vertical shear the transverse perturbations transform perturbation kinetic energy into that of the mean flow, while in our problem marginally stable disturbances of all wavelengths transfer energy from the mean flow to the perturbations. We also find that, except at low Reynolds numbers (typically $\lesssim 30$), the preferred modes generally gain more energy from the mean flow than from the release of potential energy.

This research was supported in part by the Air Force Cambridge Research Laboratory, Office of Aerospace Research, under contract F19628-67-C-0304. The computations were performed on the CDC 6400 of the University of Colorado Graduate Computing Center and on the CDC 6600 at the National Center for Atmospheric Research.

Part of this work is contained in the author's Ph.D. thesis completed at the University of Colorado under the guidance of Dr Peter A. Gilman, whose advice was greatly appreciated. The author also wishes to thank Mrs Pamela Weigle for typing the manuscript.

The National Center for Atmospheric Research is sponsored by the National Science Foundation.

REFERENCES

- ASAI, T. 1970 *J. Met. Soc. Japan*, **48**, 18.
DAVIES-JONES, R. P. 1969 Ph.D. thesis, Department of Astro-Geophysics, University of Colorado.
DAVIES-JONES, R. P. 1970 *J. Fluid Mech.* **44**, 695.
DAVIS, S. H. 1967 *J. Fluid Mech.* **30**, 465.
DEARDORFF, J. W. 1963 *J. Fluid Mech.* **15**, 623.
DEARDORFF, J. W. 1965 *Phys. Fluids*, **8**, 1027.
FRANCIS, J. G. 1961 *Comput. J.* **4**, 265.
FRANCIS, J. G. 1962 *Comput. J.* **4**, 332.
GALLAGHER, A. P. & MERCER, A. MCD. 1962 *J. Fluid Mech.* **13**, 91.
GALLAGHER, A. P. & MERCER, A. MCD. 1964 *J. Fluid Mech.* **18**, 350.
GALLAGHER, A. P. & MERCER, A. MCD. 1965 *Proc. Roy. Soc. A* **286**, 117.
HOWARD, L. N. 1963 *J. Fluid Mech.* **16**, 333.
WILKINSON, J. H. 1965 *The Algebraic Eigenvalue Problem*. Oxford: Clarendon.